value of α is close to zero, the stacking sequences are such as $a^+(h-h)a^+(c+c)c^+(h-h)c^+(c+c)b^+(h-h)b^+(c+c)a^+ \ldots$, in a concise representation *hhcchhcc...*, that is the Ti_5S_8 structure. When the value of α is close to unity, the stacking sequences are such as $a^+(c+h)b^-(c-h)a^+(c+h)b^-(c-h)a^+ \ldots$, in a concise representation *chch...*, that is the Ti_2S_3 structure. For the intermediate value of α, the intensity distribution of the faulted Ti_5S_8 structure where the $(c+c)$ layer is replaced by the $(c+h)$ layer at the probability of α and so forth is displayed among the reciprocal-lattice line $10.\zeta$ in Fig. 6. The value of ζ is twice as large as that shown in Fig. 4, because c^* is taken as equal to the reciprocal of the thickness of a layer unit.

The contents of the **P** table based on the layer units described above are easily related to the stacking sequences which are usually expressed by c and h. If y in $Ti_{1+y}S_2$ approaches zero, the partly occupied titanium layer corresponds to the van der Waals' gap between sulfur–titanium–sulfur sandwiches. In addition, these layer units can be effectively applied to depict the polytype-like phenomena observed by Tronc & Huber (1973). Then the layer units shown in Fig. 5 are convenient for considering the stacking problem in the titanium–sulfur system.

References

HENDRICKS, S. & TELLER, E. (1942). *J. Chem. Phys.* **10**, 147–167.

JAGODZINSKI, H. (1949*a*). *Acta Cryst.* **2**, 201–207.

JAGODZINSKI, H. (1949*b*). *Acta Cryst.* **2**, 208–214.

JEANNIN, Y. (1962). *Ann. Chim.* (*Paris*), **7**, 57–83.

KAKINOKI, J. (1965). *Nippon Kessho Gakkaishi* (in Japanese), **7**, 66–97.

KAKINOKI, J. (1966). *Nippon Kessho Gakkaishi* (in Japanese), **8**, 15–33.

KAKINOKI, J. (1967). *Acta Cryst.* **23**, 875–885.

KAKINOKI, J. & KOMURA, Y. (1952). *J. Phys. Soc. Jpn*, **7**, 30–35.

KAKINOKI, J. & KOMURA, Y. (1954*a*). *J. Phys. Soc. Jpn*, **9**, 169–176.

KAKINOKI, J. & KOMURA, Y. (1954*b*). *J. Phys. Soc. Jpn*, **9**, 177–183.

KAKINOKI, J. & KOMURA, Y. (1965). *Acta Cryst.* **19**, 137–147.

PATERSON, M. S. (1952). *J. Appl. Phys.* **23**, 805–811.

PATTERSON, A. L. & KASPER, J. S. (1967). *International Tables for X-ray Crystallography*, Vol. II, pp. 342–354. Birmingham: Kynoch Press.

TRONC, E. & HUBER, M. (1973). *J. Phys. Chem. Solids*, **34**, 2045–2058.

WIEGERS, G. A. & JELLINEK, F. (1970). *J. Solid State Chem.* **1**, 519–525.

WILSON, A. J. C. (1942). *Proc. R. Soc. London Ser. A*, **180**, 277–285.

Acta Cryst. (1980). A**36**, 139–142

A Simple Method to Correct for Secondary Extinction in Polarized-Neutron Diffractometry

BY R. CHAKRAVARTHY AND L. MADHAV RAO

Nuclear Physics Division, Bhabha Atomic Research Centre, Trombay, Bombay 400085, *India*

(*Received* 10 *July* 1979; *accepted* 10 *September* 1979)

Abstract

In polarized-neutron diffractometry, one often observes a variation of the polarization ratio over the rocking curve. This paper outlines a simple method which uses this interesting feature to estimate quantitatively the secondary-extinction parameter in the specimen crystal.

Introduction

In polarized-neutron diffractometry, where the aim is to obtain magnetic form factors or spin-density distributions in magnetic crystals, one has to measure with considerable precision the magnetic structure factor, M. In these experiments, M is arranged to interfere either constructively or destructively with the nuclear structure factor N (see, for example, Nathans & Pickart, 1963). Thus, for the two states of incident neutron polarization, the peak Bragg intensities are $I^+ \propto (N+M)^2$ and $I^- \propto (N-M)^2$, respectively. The measurement of the ratio of these two peak intensities, called the polarization ratio R, leads to a determination of M/N. Provided one knows accurately the nuclear structure factor, the magnetic structure factor can be directly obtained from the measurement of R. However, in the presence of extinction, the true polarization ratio R_0 will differ from the observed one R_{obs} as follows. $R_{\text{obs}} = R_0\, y^+/y^-$, where $y^{\pm}$ are the extinction

0567-7394/80/010139-04$01.00

factors applied to the integrated intensities for the two states of incident neutron polarization. It can be assumed that $y^{\pm}$ are also the correction factors to the peak intensities $I^{\pm}$ as the widths of the integrated profiles are the same for the two states of polarization and hence cancel out in the ratio measurement. Since $y^+ < y^-$, clearly the observed polarization ratio is less than the true one. Polarized-neutron experiments in crystals prone to secondary extinction have revealed several types of behaviour by $R_{\rm obs}$ over the rocking curve. In crystals like $Tb(OH)_3$ (which suffer from strong secondary extinction), $R_{\rm obs}$ was constant over the rocking curve and this was attributed to the fact that the specimen probably had type II secondary extinction (Lander & Brun, 1973). On the other hand, in many other crystals, it has been observed that the polarization ratio does vary over the rocking curve, being a minimum at the peak, increasing continuously and then attaining a steady value as one proceeds away from the rocking curve. The earliest observation of this kind was in Fe (Nathans, Shull, Shirane & Andresen, 1959) and has since been seen in several other studies, including the present one. Nevertheless, no attempt has been made so far to exploit this interesting feature to estimate quantitatively secondary-extinction effects. It is the purpose of this paper to outline a simple method of estimating the extinction parameter by illustrating its application to our observations on a single crystal of $Ni_{0.97}Ru_{0.03}$ (Madhav Rao *et al.*, 1978).

Experimental results

Several small specimens were cut by spark erosion from a large single crystal of $Ni_{0.97}Ru_{0.03}$ in the form of parallelepipeds of height approximately 8 mm, width 2 to 3 mm and thickness varying from 0·2 to 0·5 mm. In each case, the zone axis was adjusted to be along the longest dimension. The measurements of the polarization ratios were done on the polarized-neutron spectrometer at the CIRUS reactor, at room temperature in a magnetizing field of $5{\cdot}6 \times 10^5$ A m^{-1} and neutron wavelength of 0·92 Å. To facilitate extinction correction, the specimens were so cut that equivalents of the same Bragg reflection had different neutron path lengths. Polarization ratios were measured for all equivalents to a precision better than 0·2% and some of these were repeated in different zones. For the inner and therefore stronger reflections 111, 002, 220 and 113, the polarization ratios for various missets from the Bragg position were measured to detect the possible existence of secondary extinction. Fig. 1 shows a typical example of the dependence of R on Bragg misset $\Delta\omega$ for one of the equivalents of the 111 reflection. This feature shows the presence of secondary extinction and the steady extrapolated value of R for large $\Delta\omega$ should represent its extinction-free value R_0. This steady extrapolated value of R was found to be the same for all equivalents of the same reflection. That this indeed represents the extinction-free value of the polarization ratio was confirmed by a detailed analysis of the polarization ratios of all the equivalents of the 111 reflection, measured in two specimens of different thicknesses as explained below.

Analysis

As is well known, the extinction factor $y^{\pm}$ is a function of the quantity $Q^{\pm}\,\bar{T}$, where $\bar{T}$ is the effective neutron path length in the crystal and $Q^{\pm}$, the integrated reflectivity, is defined as $Q^{\pm} = (N \pm M)^2\,\lambda^3/V^2 \sin 2\theta$. V is the volume of the unit cell, N and M are the nuclear and magnetic structure factors, respectively. (In all our discussions, we assume that the 'peak' intensities that we measure at the peak of the rocking curve are proportional to the corresponding integrated reflectivities. This is a valid assumption since the profile widths do not change.) We define the 'extinction-free' or true polarization ratio R_0 as the steady extrapolated value of $R_{\rm obs}$ as shown in Fig. 1. Here, $R_0 = 1{\cdot}410$. Since the incident-beam polarization and the RF flipper efficiency are close to unity, we write

$$R_{\rm obs} = R_0\,y^+/y^- = [(N+M)^2/(N-M)^2](y^+/y^-),$$

$$y^+/y^- = R_{\rm obs}/R_0. \qquad (1)$$

Polarization ratios in the reflection (r) and transmission (t) geometry and also at various Bragg missets were measured in two specimens of different thicknesses (0·6 and 0·3 mm). Thus, corresponding to the zero Bragg misset measurements, four relations of the form (1) can be written down:

$$y(Q^+\bar{T}_i)/y(Q^-\bar{T}_i) = (R_i)_{\rm obs}/R_0, \qquad (2)$$

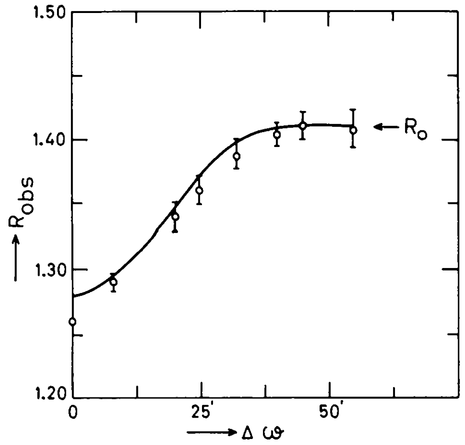

Fig. 1. The polarization ratio (open circles) measured for the 111 reflections at various Bragg missets in specimen 2 in transmission geometry. The solid curve is the calculated polarization ratio (see text for explanation).

Table 1. *Summary of the peak observations in the* 111 *reflection for two specimens of thicknesses* 0·6 *and* 0·3 mm

$Q\bar{T}$ is in units of 10^{-4}.

Specimen	Geometry	Path length, $\bar{T}$, in mm	$Q^+\bar{T}$	$Q^-\bar{T}$	R_{obs}	R_{obs}/R_0
1	Transmission (t_1)	0·576	10·4	7·1	1·257 (2)	0·891
	Reflection (r_1)	1·682	30·5	20·8	1·217 (2)	0·863
2	Transmission (t_2)	0·291	5·3	3·6	1·261 (2)	0·894
	Reflection (r_2)	1·038	18·8	12·8	1·221 (2)	0·866

where i runs over four values, two relative to transmission and two relative to reflection geometry. From the known value of R_0 (=1·410) and knowing N, the nuclear structure factor, the reflectivities $Q^\pm$ and thus $Q^\pm\,\bar{T}$ for each of these reflections were calculated (the path lengths $\bar{T}$ were numerically computed). The effective path lengths $\bar{T}$, the parameters $Q\bar{T}$ (for the + and − states of the incident-beam polarization) and $(R_i)_{obs}$ are shown in Table 1.

Since we now have four relations in the form of (1), it is a simple matter to estimate the extinction parameter g, provided we assume some analytical form for the extinction factor y. We have used Zachariasen's (1967) formula for type I secondary extinction:

$$y = (1 + 2gQ\bar{T})^{-1/2}. \tag{3}$$

Equation (1) is then recast in the following form

$$\frac{(R_i)_{obs}}{R_0} = \left[\frac{1 + 2gQ^-\,\bar{T}_i}{1 + 2gQ^+\,\bar{T}_i}\right]^{1/2}. \tag{4}$$

The only unknown quantity in this equation is the extinction parameter g. The four observed polarization ratios were least-squares fit with (4) to obtain the extinction parameter g. These calculations were performed on a desk calculator and g was found to be $(0{\cdot}11 \pm 0{\cdot}01) \times 10^4$. It is worthwhile recalling that a full-matrix least-squares analysis using a computer program carried out on all the 70 measured polarization ratios, including all equivalents (Madhav Rao *et al.*, 1978), using Zachariasen's formula yielded a g value of $0{\cdot}13 \times 10^4$ which is fairly close to the value we get by the present simple analysis.

In order to satisfy ourselves about the reliability of this procedure, we have tested it against four more reflections, 002, 220, 113 and 333, where the polarization ratios R_{obs} at the peak ($\Delta\omega = 0$) and R_0, the polarization ratios at large $\Delta\omega$ are measured. Since we have defined R_0 to be the extinction-free polarization ratio, it is straightforward to calculate (as is explained earlier for the 111 reflection) the reflectivities $Q^\pm$. With a knowledge of the path lengths $\bar{T}$, and using the same value of g ($=0{\cdot}11 \times 10^4$) obtained from the analysis of the 111 reflections, we used (4) to calculate the polarization ratio at the peak for these four reflections. These results are assembled in Table 2, where the observed peak polarization ratios are shown in column 3, and the calculated ones based on the present analysis are shown in column 4. By way of comparison, we have shown in the last column the calculated peak polarization ratios obtained from a full-matrix least-squares analysis of all the measured reflections (Madhav Rao *et al.*, 1978). Except perhaps for the 002 reflection, where the discrepancy between the observed and calculated values is not negligible, the agreement is found to be quite good.

Finally, we wish to explain quantitatively the variation of the observed polarization ratio for various Bragg missets in the 111 reflection. In Fig. 1 are plotted the observed polarization ratios (R) for various $\Delta\omega$ of specimen 2 in transmission geometry. This variation of R essentially arises from the variation of the reflectivity, Q, over the rocking curve, with g and $\bar{T}$ remaining constant. To a very good approximation, we assume the reflectivity $Q_{\Delta\omega}$ at any $\Delta\omega$ to be given by

$$Q_{\Delta\omega} = Q \exp(-\Delta\omega^2/2\sigma^2), \tag{5}$$

where Q is the reflectivity at the Bragg position (see Table 1) and σ is the true dispersion of the rocking curve. In Fig. 2 is shown the background-corrected rocking curve measured for the + state of the incident-beam polarization (the FWHM of the rocking curves for the + and − neutron spin state are the same). It is important to emphasize here that the measured dispersion of the rocking curve can, in general, be differ-

Table 2. *Summary of the observed peak polarization ratios and the calculated polarization ratios*, R_{cal}(I), *based on the present analysis with* $g = 0{\cdot}11 \times 10^4$

R_{cal}(II) are the calculated polarization ratios from the full-matrix least-squares analysis of all the 70 measured reflections using a computer program (Madhav Rao *et al.*, 1978).

Reflection	R_0	R_{obs}	R_{cal} (I)	R_{cal} (II)
002	1·366	1·228	1·251	1·240
220	1·202	1·141	1·140	1·141
311	1·144	1·113	1·110	1·111
333	1·048	1·037	1·037	1·037

ent from the true one. The following equation gives the relation between these (Sequeira, 1974).

$$\sigma_{\text{meas}} = \sigma\left[\frac{\alpha_2^2+\delta^2}{\alpha_2^2+\delta^2+g_1^2\sigma^2}\right]^{1/2}. \qquad (6)$$

α_2 is the counter collimation, δ and g_1 are instrumental parameters whose full expressions have been given by Sequeira (1975). It is thus straightforward to calculate the true dispersion from the measured one for any spectrometer. On our polarized-neutron spectrometer, we found that the term in the square bracket of (6) was essentially unity and the true dispersion of the rocking curve was 12′. Knowing Q^+ and Q^- at the Bragg position to be 0·00182 and 0·00124 mm^{-1}, respectively, we calculated $Q^{\pm}_{\Delta\omega}$ for the various $\Delta\omega$'s using (5). The polarization ratio R at any given $\Delta\omega$ was calculated using (4):

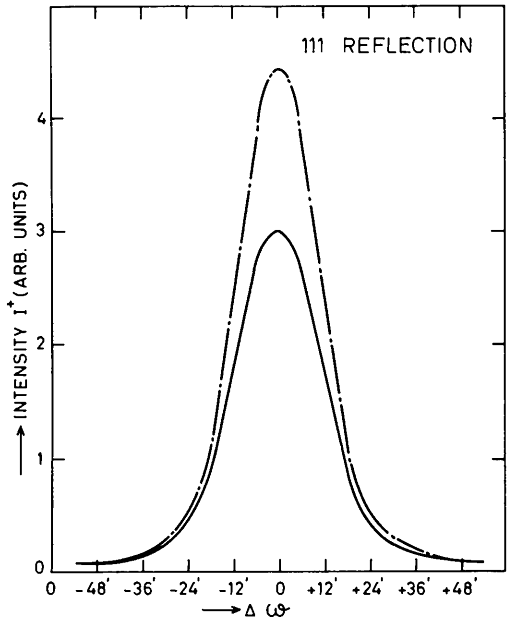

Fig. 2. The continuous line is the background-corrected rocking curve measured in the + neutron spin state for the 111 reflection for specimen 2 in transmission geometry. The broken line is the extinction-corrected rocking curve.

$$R = \left[\frac{1+2gQ^-_{\Delta\omega}\bar{T}}{1+2gQ^+_{\Delta\omega}\bar{T}}\right]^{1/2} \times 1{\cdot}410,$$

with $g = 0{\cdot}11 \times 10^4$ and $\bar{T} = 0{\cdot}291$ mm. This calculated polarization ratio is shown as a continuous curve in Fig. 1. No least-squares was done in this region, so the agreement between the observed polarization ratios and the calculated ones is seen to be very good.

Conclusion

We have been able to demonstrate that in magnetic crystals suffering from secondary extinction, the polarization ratio, R, measured at high Bragg missets represents its extinction-free value and its variation across the rocking curve can be quantitatively explained in terms of a single extinction parameter. In an actual spin density and form-factor study, where the polarization ratios of a large number of reflections have to be measured with great precision, it is quite useful to measure also the polarization ratio at large Bragg missets. The present analysis then affords a quick and reliable method of estimating extinction in the crystal.

We are grateful to Dr N. S. Satya Murthy for his interest and encouragement in this work and to Dr A. Sequeira for useful discussions.

References

Lander, G. H. & Brun, T. O. (1973). *Acta Cryst.* A**29**, 684–691.

Madhav Rao, L., Chakravarthy, R., Jirak, Z. & Satya Murthy, N. S. (1978). *Phys. Rev. B*, **18**, 6275–6282.

Nathans, R. & Pickart, S. J. (1963). In *Magnetism*, Vol. III, edited by G. T. Rado & H. Suhl, pp. 211–269. New York: Academic Press.

Nathans, R., Shull, C. G., Shirane, G. & Andresen, A. (1959). *J. Phys. Chem. Solids*, **10**, 138–146.

Sequeira, A. (1974). *Acta Cryst.* A**30**, 839–842.

Sequeira, A. (1975). *New Methods and Techniques in Neutron Diffraction*. Report No. RCN-234, Petten.

Zachariasen, W. H. (1967). *Acta Cryst.* **23**, 558–564.